Published in Filtech 2003, Düsseldorf

Simulation of fluid particle separation in realistic three dimensional fiber structures

A.Latz, A. Wiegmann
Fraunhofer Institut für Techno- und Wirtschaftsmathematik,
Gottlieb-Daimler Str. 67663 Kaiserslautern, Germany

July 16, 2003

Abstract

Methods from stochastic geometry allow to construct models which are very good representations of the real complexity of Nonwovens. These realistic models are used as boundaries for a fluid dynamic simulation with a parallel Lattice Boltzmann code, developed by the Fraunhofer ITWM in recent years. As a result, the flow field, the pressure drop across the filter and its permeability are obtained. To study the depth filtration properties, we used a Lagrangian formulation of particle transport in the calculated complex flow field. The relative influence of different filtration mechanisms and the filtration efficiencies of the complex fiber structures are studied as function of particle sizes ranging from $D = 2\mu m.$ to $4nm$. The most penetrating particle size is obtained in good agreement with experiments. For larger particles the clogging of the filter is studied. As an interesting phenomenon, we find often an inhomogeneous loading for particles, even if the particle size is appreciable smaller than typical pore sizes.

Keywords: models for complex fibrous microstructures, Lattice Boltzmann simulation, Simulation of sieving effect, Filter Efficiencies, Filter Clogging, Flow in complex structures, Depth filtration, Filter Loading, Particle Separation, Nonwovens

1 Introduction

The interplay between the microstructure of fibrous filter media and the functionality of the resulting filter (pressure drop, permeability, filter efficiency, Filtration ratio) is of considerable practical importance. There is a vast literature on single fiber theory and many ansatzes to obtain informations about the filter as a whole [1, 2, 3, 4]. But in these, simplifying ansatzes like introducing very regular structures, are necessary to obtain results. Real fibrous filters on the other side have a very complicated microstructure. Therefore this models are not sufficient for large particles and small particles as well. If the particle sizes become comparable with the pore sizes the filtration is dominated in most cases by inertia effects, which depend strongly on the flow field, and, much more important, on the irregular distribution of available free space for the particles to penetrate. Particles are captured due to sieving and e.g. get caught in corners formed by irregular three dimensional arrangement of fibers, not present in regular structures.

But also in the case of small particles the filtration properties of a single fiber or a regular (periodic) arrangement of fibers can be very different compared to real fibrous structures even if the porosity is the same. This is again due to the very different flow fields compared to periodic structures, if inertia is the dominant filtration mechanism. And even in the case of very small particles for which Brownian motion is the dominant filtration mechanism, the flow field influences characteristically the capture of particles [5].

2 Methods

To study the details of the particle filtration process in technical textiles and paper we need a faithful representation of the complex geometries of Nonwovens and different papers, the techniques to calculate the fluid flow through these microstructures and an algorithm to study the interaction of particles with the flow and the fibers. The irregular three dimensional structure of Nonwovens can be modeled with the help of methods from stochastic geometry [6, 7]. These methods allow to generate structures with prescribed distribution of fiber diameters, fiber orientations and porosities. Also the form of the fibers (cylinder, ellipsoid, trilobal cross sections etc.) can be selected [8]. Once the structure is generated its flow properties have to be calculated. To do this, we took the Lattice Boltzmann approach to solve the incompressible Navier Stokes equation [9]. To be able to calculate the flow in large complex geometries, we used a parallelized Lattice Boltzmann Code, which was developed in recent years by the Fraunhofer ITWM especially for industrial applications [10, 11, 12, 13, 14]. With the help of this code not only the three dimensional flow field $\vec{\mathrm{v}}(\vec{r})$ but also the permeability tensor of the complex micro structure is calculated.

The dynamics of particles is determined by solving the equation of motion for a collection of non interacting particles, which are coupled to the flow, exposed to the thermal fluctuations of fluid molecules and, in addition, can interact with the fibers. All these effects can be described by a stochastic differential equation for the position $\vec{r}(t)$

and the velocity $\vec{u}(t)$ of the particles

$$\frac{d\vec{r}}{dt} = \vec{u}(t) \quad (1)$$

$$d\vec{u} = -\gamma(\vec{u}(t) - \vec{\mathsf{v}}(\vec{r}(t)))dt + \sigma * d\vec{W}(t) \quad (2)$$

$$\langle dW_i(t)dW_j(t)\rangle = \delta_{ij}dt \quad (3)$$

Here γ is the friction coefficient due to the kinematic viscosity ν, fluid mass density ρ_F and particle mass density ρ_p:

$$\gamma = \frac{3}{8}\frac{\rho_F}{\rho_p R_p} c_d \; * |\vec{u}(t) - \vec{\mathsf{v}}(\vec{r}(t))| \quad (4)$$

with the drag coefficient $c_d = f(Re_p)$ being a function of the Reynolds number of the particle Re_p with radius R_p:

$$Re_p = 2R_p \frac{|\vec{u}(t) - \vec{\mathsf{v}}(\vec{r}(t))|}{\nu} \quad (5)$$

In the case of pure Stokes flow ($Re_p < 0.1$), which is fulfilled in all examples used here, the drag coefficient is given by $c_d = 24/Re_p$. The stochastic force in (2) is given by the product of a three dimensional Wiener process $d\vec{W}(t)$ with variance 1 and the variance σ, which is given by

$$\sigma^2 = 2\gamma \frac{3k_BT}{4\pi\rho_p R_p^3} \quad (6)$$

with k_B, T being the Boltzmann constant and the temperature, respectively. As usual, the first term in (2), proportional to the absolute value of the difference of the local fluid velocity $\vec{\mathsf{v}}(\vec{r}(t), t)$ and the velocity of the particle $\vec{u}(\vec{r}(t), t)$, will give rise to the inertia mechanism of filtration, where the second term $\propto 1/R_p^{5/2}$ is responsible for the Brownian fluctuation mechanism of filtration.

To complete the description of particle motion we need a model for the interaction of particles with the fibers. At the present stage we consider particles which collide inelastically with the fibers, loosing momentum and energy at every contact with a fiber. I.e. the velocity of a particle $\vec{u}'$ after contact with the fibers is given by

$$\vec{u}' = r_t * (\vec{u} - (\vec{n} * \vec{u})\vec{n}) - r_n(\vec{n} * \vec{u})\vec{n} \quad . \quad (7)$$

The parameter $0 \leq r_t, r_n \leq 1$ quantify the relative loss of momentum tangential and perpendicular to the collision plane. The vector $\vec{n}$ is the collision normal perpendicular to the collision plane. Since contact with several fibers is possible the collision plane is constructed from all contact points, taking the different orientation of the fibers into account, with which the particle is in contact. If $r_t = r_n = 1$ the collision would be completely elastic. In the following examples we consider the case where $r_n = r_t = 0.2$ i.e. there is 80% loss of momentum at the collision. This approach is necessary to avoid the unphysical situation, that particles with sizes comparable to the fiber thickness are caught by a single fiber already at first contact, even if their motion where tangential to the fiber. Capturing of those large particles is in our model only possible if they hit one fiber practically head on or if they are caught from crossed fibers like in a sieve. Small particles can get caught also from a single fiber since they have to get so close to the fiber, that due to the boundary layer around the fibers, the fluid velocity is too small to cause an acceleration and therefore detaching of the small particles. Adhesion can be easily modeled within this approach by introducing a threshold force, which has to be overcome to detach from the fibers again.

3 Results

Figure (1) shows an example of a fiber geometry with a slightly preferred orientation perpendicular to the main axis. The geometry consists of $128 \times 128 \times 256$ voxels. This also defines the discretization of the Lattice Boltzmann calculation i.e. one voxel edge length corresponds to one Lattice Boltzmann unit (LB unit). The fibers have a diameter of three LB units, the total solid volume fraction is exactly 10%.

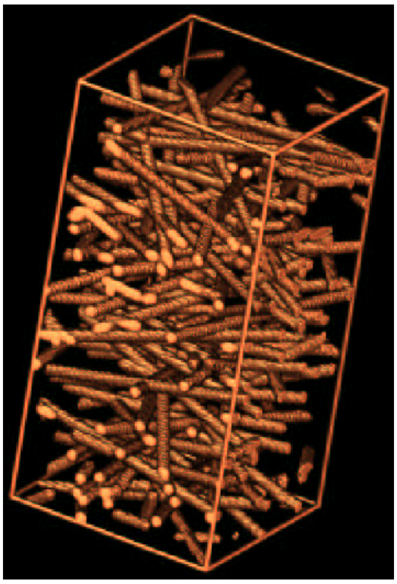

Figure 1: Fiber geometry $128 \times 128 \times 256$ voxels. The fibers have a radius $R_F = 3$ LB units.

By applying a small pressure gradient in the z - direction of the geometry (the longest axis), a flow is initiated. The Reynolds number of the flow $R_e = v_{max} D_p / \nu_{LB}$, defined by the maximal velocity v_{max} of the flow, the diameter $D_p = 2R_p$ of the fibers and the scaled kinematic viscosity ν_{LB} is well in the Stokes regime ($R_e \approx 0.01$). To give a physical example, we identify one LB unit with one μm, the fluid should be air with a kinematic viscosity of $\nu = 9.4 * 10^{-7} m^2/s$ and a density of $\rho_F = 1.229 kg/m^3$. In this case the maximal velocity is $v_{max} = 0.0435 m/s$.

For the same geometry we calculated the filtration efficiency for particles with diameters ranging from $2\mu m$ to $4nm$. To achieve this, we followed the motion of 5000 particles for each diameter with two different initial conditions for each particle by solving the stochastic differential equations (1,2). The mass density of a single particle was assumed to be $\rho_p = 2580 kg/m^3$. As a measure for the filtration efficiency E we used the ratio N_T/N of particles caught to the total number of particles normalized to the total time of calculation t.

$$E = -\frac{\log(N_T/N)}{t} \tag{8}$$

This normalization is necessary to be able to compare the different runs for the different particle sizes. Fig. (2) shows the result of the calculation.

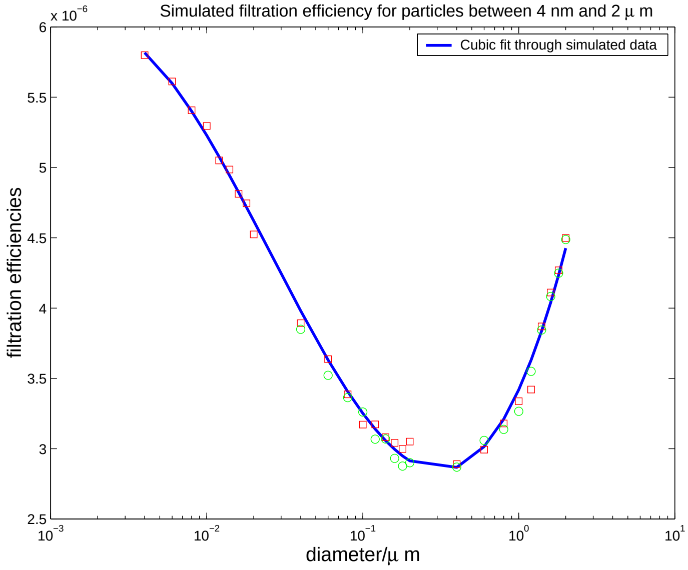

Figure 2: Filter efficiency as defined in (8) as a function of the particle diameters. The different symbols are the results of simulations for different initial conditions. The solid line is a cubic fit through the data.

We obtain exactly the expected behavior e.g. a cross over from a regime at larger values of the diameter dominated by inertia to a regime where Brownian motion is responsible for the filtration. Their is a well defined most penetrating particle size of $D_{pen} \approx 0.4\mu m$. This value is at the given flow velocities in very good agreement with experiments [1, 15, 16].

To study the clogging of filters we took for demonstrating purposes a smaller geometry ($64 \times 64 \times 128$). The solid volume fraction ($= 0.1$) and radius of the fibers ($R_F = 3\mu m$) is chosen as before. But contrary to before we concentrate on particles with radius $R_p = 6\mu m$. In this case particles can still go easily through the filters but some are caught in corners of crossing fibers and start to change the flow. Figure (3) shows a snapshot where two particles are caught by the sieving effect. As can be seen clearly there seems to be enough free space for particle to penetrate. Yet, after several cycles of iteratively capturing particles and recalculating the flow, the final configuration looks very asymmetric as can be seen in Fig. (4). In this configuration it is not possible to place another particle at the entry of the filter section i.e. a filter cake starts to form. One can identify a pair of particle, which was able to penetrate deeply into the filter, but the bulk of particles is caught at the entry (i.e. at the top of the figure).

The total permeability of the filter section at the end of the clogging simulation is less than half of the one at the beginning and the solid volume fraction increased from 0.1 to 0.195. Fig. (5) shows the development of the permeabilities during the clogging

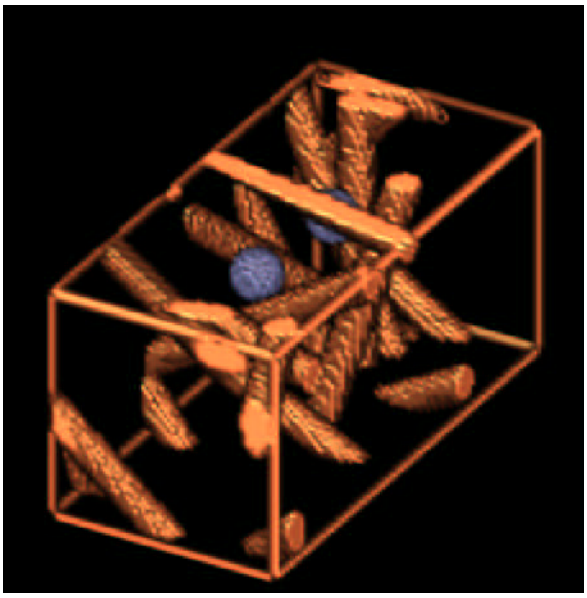

Figure 3: Two particles of radius $R_p = 6\mu m$ caught in a filter section of size $64\mu m \times 64\mu m \times 128\mu m$. The radius of the fibers is $R_F = 3\mu m$. The flow is from front to back

Figure 4: Final configuration before a cake starts to form. The flow is from top to bottom.

process against the actual solid volume fraction. We also show an estimate of the permeability of the clogged region at the entry only. Under the condition of constant mass flux through the filter and assuming a linear relation between inverse permeability and pressure drop, this shows that the mechanical stress in the clogged region is about

4 times as high as for the unloaded filter. We also calculated the permeability of a configuration with the same solid volume fraction as the clogged filter, but an homogeneous distribution of dirt particles. This homogeneous configuration has a comparable total permeability but due to its homogeneity the pressure drop is distributed over the whole filter. In addition it is still possible to catch particle within the homogeneous filter, whereas in the clogged filter a filter cake starts to grow.

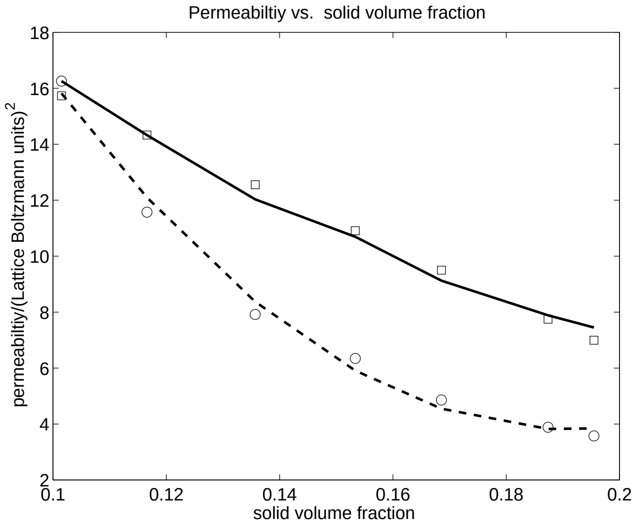

Figure 5: The solid line shows the development of total permeability during the clogging process. The dashed curve is an estimate for the permeability of the clogged region of the filter, which can be unambiguously identified in Fig. (4).

4 Conclusions

We have demonstrated that it is possible to calculate the flow as well as the filtration properties (efficiency, clogging behavior) of realistic three dimensional fiber structures with the help of methods from stochastic geometry and Lattice Boltzmann simulation techniques. Since controlled variations of structural parameters like fiber orientation, form of the fibers, spatially varying pore size distribution or gradients in the fiber density can easily achieved within the simulation, our results constitute a systematic and quantitative approach for the calculation of the fluid particle separation in fibrous filters.

References

[1] R.C. Brown, “Air Filtration, An Integrated approach to the Theory and Application of Fibrous Filters”, Pergamon Press, Oxford (1993).

[2] K. Spurny (Ed.), “Advances in aerosol filtration”, CRC Press LLC (1998).

[3] O. Filippova, D. Hänel. “Lattice-Boltzmann Simulation of Gas-Particle Flow in Filters”, Computer & Fluids, vol 7, pp. 697-712, (1997).

[4] W. Bergmann, I. Corey, “Filtration Theory using Computer Simulations”, 24th DOE/NRC Nuclear Air Cleaning and Treatment Conference (1996).

[5] A. Latz, 2. Bericht zum Projekt der Stiftung Rheinland-Pfalz für Innovation, “Partikel und Wärmetransport durch Strömungen in Mikrostrukturen” (2003).

[6] J. Ohser u. F. Mücklich, “Statistical Analysis of Microstructures in Materials Science”, John Wiley & Sons (2000)

[7] Fraunhofer Institut für Techno- und Wirtschaftsmathematik, Jahresberichte 2000 - 2002.

[8] “The optimal stuff”, Fraunhofer Gesellschaft Research News No.4 (2003).

[9] S. Succi, Lattice Boltzmann Equation for Fluid Dynamics and Beyond (Numerical Mathematics and Scientific Computation), Oxford University Press (2001).

[10] I. Ginzburg, P. Klein, C. Lojewski, D. Reinel-Bitzer, K. Steiner, Parallele Partikelcodes für industrielle Anwendungen,Verbundprojekt im Rahmen des HPSC, Abschlussbericht ITWM Kaiserslautern, März 2001.

[11] I. Ginzburg u. K. Steiner, “A Lattice Boltzmann model for free-surface flow and its application to filling process in casting”, J. Comp. Phys., **185**, 61 (2003)

[12] I. Ginzburg u. K. Steiner, “A free-surface Lattice Boltzmann method for modeling the filling of expanding cavities by Bingham fluids”, Phil. Trans. R. Soc. Lond. A , **360**, 453 (2002).

[13] I. Ginzburg, D. d’Humieres, “Multi-reflection boundary conditions for lattice Boltzmann models”, preprint (2002).

[14] D. Kehrwald, “Numerical Analysis of Immiscible Lattice BGK”, Dissertation, Universität Kaiserslautern (2002).

[15] J. W. Thomas, R. E. Yoder, Aerosol size for maximum penetration through fiberglass and sand filters, AMA Arch. Ind. Health **13**, 545 (1956).

[16] J. Dyment, Use of Goertz aerosol spectrometer for measuring the penetration aerosols through filters as a function of particle size, Aerosol Sci., **1**, 53 (1970).